Crack Patterns Induced by Foundation Settlements: Integrated Analysis on a Renaissance Masonry Palace in Italy

Claudio Alessandri,[1] Massimo Garutti,[1] Vincenzo Mallardo,[2] and Gabriele Milani[3]

[1]*Department of Engineering, University of Ferrara, Ferrara, Italy*

[2]*Department of Architecture, University of Ferrara, Ferrara, Italy*

[3]*Department of Architecture, Built Environment and Construction Engineering, Technical University of Milan, Milan, Italy*

1. INTRODUCTION

The geographic area including the city of Ferrara (north of Italy) is characterized by soft and very soft soil layers, such as clay with loam, and, more rarely, with sand. In the historical masonry structures of such an area it is rather common to find crack patterns that testify differential settlements that are still in progress or have already occurred—the absence of signifi-cant seismic events (before 2012) in the past 500 years confirms such a statement. The poor mechanical characteristics of the soil may cause differential settlements even in the new masonry structures that have been designed with insufficiently rigid and strengthened foundations.

Gulinelli Palace (also known as *Palazzo Contughi Gulinelli*) in Ferrara, Italy, has been subjected to many structural modifications over time since its construction. Such modifications are probably the main causes that have produced remarkable stress states and the consequent occurrence of evident crack patterns.

The issue of the determination of the crack patterns caused by the differential settlements has been studied as a "direct problem" for a long time. The original research by Skempton and MacDonald (1956) and then by Grant, Christian, and Vanmarcke (1974) as well as the work still in progress, demonstrates the early interest of the scientific community to this topic.

The earliest studies mainly provided a measure of the maximum allowable settlements to be borne by the structure without significant damage. Such results were supported by the onsite observation of the real structures and not by numerical or theoretical results. Although they are now a bit out-of-date, they still represent a valid design tool for professionals, both engineers and architects, and, at the same time, a demonstration of the difficulty in developing new and more efficient procedures. Surely the spread of the numerical methods, such as the finite element method (FEM) or the boundary element method (BEM) have provided new very effective tools of investigation.

Very recently, particular attention has been devoted to the tunneling excavation problem, as in Janda, Sejnoha, and Sejnoha (2013), a study for which FE models were applied on the upper structure in combination with a semi-analytical approach for the soil, or in Giardina et al. (2012), a study for

Received September 30, 2013; accepted February 1, 2014. Address correspondence to Gabriele Milani, Department of Architecture, Built Environment and Construction Engineering (A.B.C.), Technical University of Milan, Piazza Leonardo da Vinci 32, 20133 Milan, Italy. E-mail: gabriele.milani@polimi.it

which both laboratory tests and numerical analyses were carried out to measure the effects induced on the facade of a masonry structure by a tunnel excavation. This attention notwithstanding, the inverse problem to identify the location and the entity of the settlement on the basis of the surveyed crack pattern is still an open issue.

The structural analysis of historical buildings with attention to the damage caused by known differential settlements has been studied even in the past decades. In Alessandri and Mallardo (2012) and Alessandri et al. (2012), the investigation is focused on the crack pattern surveyed on the bearing walls of the Church of Nativity in Bethlehem. In Padura et al. (2012), the foundations and the bearing soil of the Giralda minaret of Seville are investigated. This study mainly focus on the direct problem to simulate the settlements occurred at the base of the minaret over its 800 years of life and to simulate the circumstances in which the tower settlement would have generated the foundation collapse.

In Gikas and Sakellariou (2008), the long-term settlement of the Mornos dam is simulated by means of a FE analy-sis and the use of some vertical displacement data. It is an attempt to solve the inverse problem linking the visible effects with the actual causes. In this way, measured deformations resulting from a continuous geodetic monitoring are used to recover the deformation history with the aid of some numerical analyses.

It must be pointed out that the correct identification and quantification of the settlements provoking some visible crack patterns is extremely helpful in establishing the minimum and most correct intervention of rehabilitation, and in guaranteeing the sufficient strength and stiffness to cope with rarer and severe actions such as the seismic ones. The issue concerning the ancient masonry structures is complicated by the frequent inner disconnection of their components, which increasingly complicates the numerical modeling. Furthermore, the mechanical and numerical modeling of cracks occurring and propagation in brittle structure requires complex procedures that are still under progress as reported in the scientific literature (for exam-ple, Holl, Loehnert, and Wriggers [2013] in the extended FEM context and Mallardo [2009] in the BEM context).

For these reasons, in the present study the authors intend to focus on the identification of location and entity of the foundation settlements that, in their opinion, may have caused the visible crack pattern of the facade (Figure 1). As described in more detail in the next section, such settlements might have occurred in consequence of the addition of some floors on one side of the building and, on the other side, of new loads transferred by the adjacent building. Therefore the present work can be considered as an attempt to solve the inverse problem of the definition of the possible causes of a structural damage on the basis of some surveyed data.

The whole procedure carried out to achieve the desired results can be considered as an integrated analysis since it involves various research fields, such as the study of the historical documentation concerning the Palace, the geometrical and structural survey, the monitoring of the damage, the numerical simulation by means of standard and ad hoc FE codes. The comparative analysis of all the information obtained from different sources allows to narrow the field of the possible solutions to a given problem by matching as much as pos-sible the different data and satisfying at best the imposed conditions.

In Section 2, a short history of Palazzo Gulinelli is reported from the date of its construction up to the last century with a special focus on the structural modifications occurred over time, the last of which considered by the authors as one of the causes of the crack pattern on the facade. Section 3 is a description of the load-bearing structures of the building, of the crack pattern surveyed on the façade, and of the data obtained by monitoring three different cracks over a period of approximately 1 year. The correspondence between one set of such data and the different times of the year is particularly interesting. It is worth noting that the main beams of the first two floors are parallel to the facade and therefore they are not able to pre-vent or reduce possible out-of-plane movements of the facade, which, in consequence, becomes more vulnerable to seismic actions.

Also in Section 3, the whole building in its present configuration is analyzed by using a FE model within the Straus code with the aim of defining the internal stress state produced by

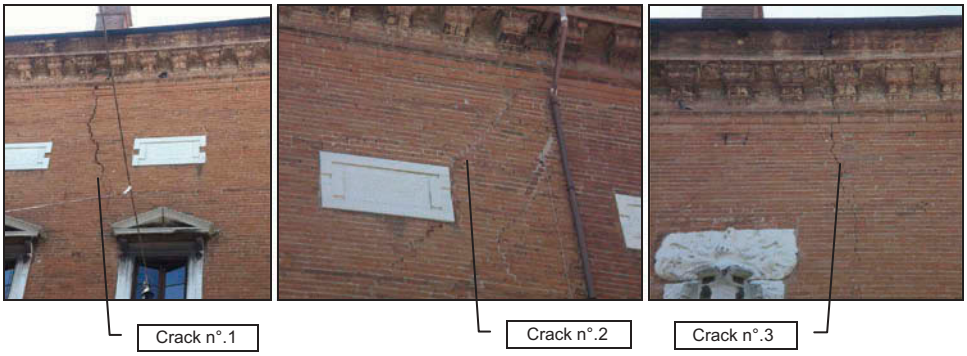

FIG. 1. Gulinelli Palace, showing the crack pattern on the main facade.

the gravity loads and the foundation settlements. Two different approaches are followed: the first is linear elastic; the sec-ond is elastic-plastic with a Mohr-Coulomb criterion assumed at failure for masonry. The soil under the structure is mod-eled by means of Winkler-type elastic springs, which assume different stiffness values according to the hypothesized differ-ential settlements. Both approaches give rise to results in terms of principal stresses and vertical displacements, which match very well the existing crack pattern, confirming that the present state of damage may be ascribed to differential settlements in correspondence of the foundation level.

Sections 4 and 5 present the main features of a non-linear FE procedure based on a homogenized FE approach, first presented in Milani (2011), and suitable to analyze complex masonry structures in the non-linear range, specifically by taking into account the material anisotropy and the softening behavior on tension. The structural model relies on a discretization with rigid triangular elements and non-linear interfaces. Cracks prop-agation, if any, is therefore constrained to occur between con-tiguous elements. The procedure consists of two main steps: in the first place masonry is replaced by a fictitious homogeneous material by solving in the non-linear range a boundary value problem on a suitable representative element of volume (REV). Section 6 in particular provides an insight into the inelastic behavior of a typical REV of the Palace analyzed according to the non-linear homogenization approach described in the paper.

In the end the inelastic behavior obtained for a REV is implemented at a structural level and extended to the whole structure, as described in Section 7.

The entire homogenization procedure is then implemented in Section 8 in a discretized model of Palazzo Gulinelli including a Winkler elastic soil characterized by springs with discontinuous values of their stiffness. A parametric analysis, carried out on the basis of the structural survey and of the monitoring data, shows that the surveyed crack pattern can be repro-duced with a good approximation by using only two different values for the spring stiffness, suitably distributed along the base of the building. The numerical results obtained by using commercial FE codes, homogenized FE models, and rather sim-plified models are compared and tested with the surveyed crack pattern. A good agreement among all of them can be envis-aged; that proves the reliability of the non-linear homogenized FE approach in analyzing even complex masonry structures and supports the hypothesis of a tight relationship between differential settlements and existing crack pattern.

A discussion of the experimental and numerical results (Section 9) and some final considerations (Section 10) about the goals achieved, in particular the good matching between numer-ical and monitored data, the advantages of an integrated analysis like the one here carried out and the prospects of future research, conclude the article.

2. HISTORICAL DESCRIPTION OF THE PALACE

The Palace, commissioned by Girolamo Mario Contughi and built in 1542 (Torboli 1999), is an historic and compact building with load-bearing masonry walls, consisting of four stories, one of which is the basement (Figure 2). It hosted the Department of Human Sciences of the University of Ferrara for many years but it was closed at the beginning of 2012 (before the relevant seismic event of May 2012), for safety reasons, in consequence of the worrying crack pattern that had occurred over time. The Palace was not built in one step, but instead it is the result of the recast of more preexisting buildings, as shown by some inhomogeneities in the facade and irregularities in plan and height. The analysis of the map of the basement (Figure 2b) suggests

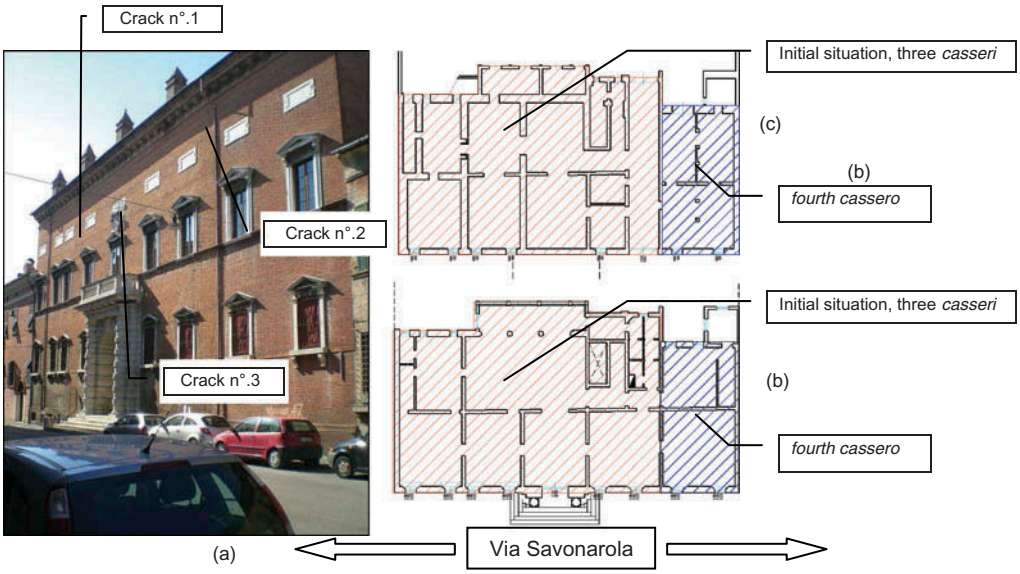

FIG. 2. Gulinelli Palace: (a) main facade, (b) basement, and (c) first floor.

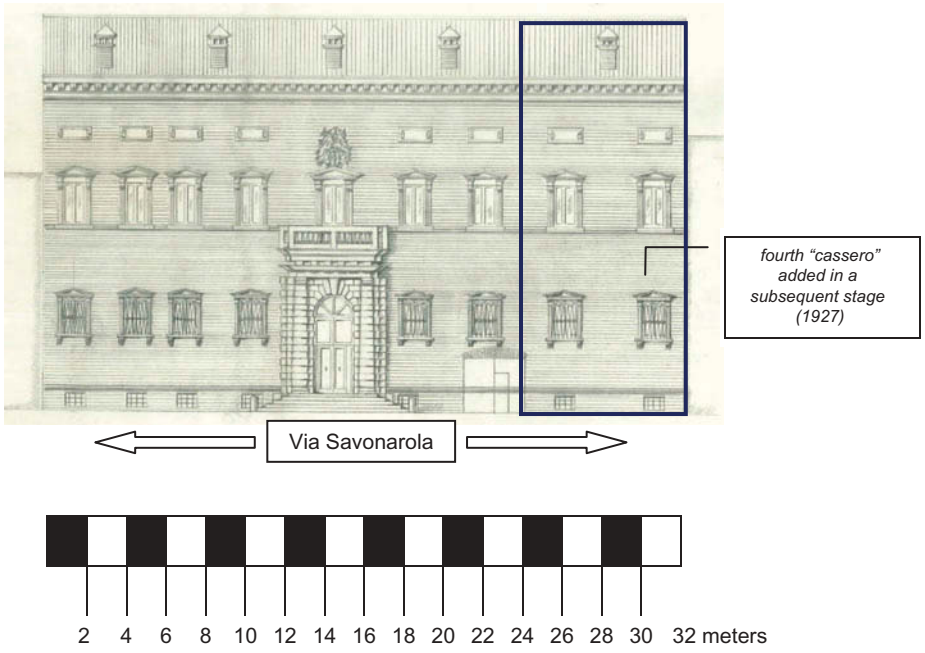

FIG. 3. The main facade on via Savonarola.

FIG. 4. The original facade and the corresponding one on the rear before the 20th century.

that the original structure was a compound of three *casseri*, the first three parts moving from the left to the right in Figure 2, Figure 3, and Figure 4 (where the term *cassero* stands for the typical unit building in Ferrara at that time and it is enclosed in two parallel continuous walls), plus a service wing. The por-tal was added at a later stage and it is commonly ascribed to Balbi on the basis of a stylistic comparison with the por-tal of Palazzo Paradiso, a coeval building located in the city center.

3. STRUCTURAL SURVEY AND DIAGNOSIS

The geometrical and structural survey carried out by the authors of the current study, in addition to the survey performed by Laudiero (2009), allowed to define the wall thicknesses, the beam layout of the floors and the crack pattern. The vertical structure of the building consists of load bearing masonry walls made of one-, two-, three- and four-head (at the basement) solid brick walls (see Figure 5: in red and in blue the four-head and the two-head masonry walls respectively, measurements are in meters). The floors are composed of a two-dimensional (2D) grid of wooden beams (Figure 6, photo n° 8), except some floors at the first floor supported by masonry vaults and some other floors supported by steel beams and more recently refurbished.

No information about the foundations is available. On the basis of the data available from other nearby historical palace, it may be supposed that the foundations are a prosecution of the visible walls with gradual and successive enlargements.

The Palace as a whole presents a diffused crack pat-tern. Very probably it can be ascribed to the differen-tial settlements occurred over time because of the numerous structural modifications and functional changes in the building.

On the basis of the survey carried out, it is possible to state that the main facade on Via Savonarola (Figure 2–4) is one of the most vulnerable parts of the Palace. This vulnerabil-ity is demonstrated both by the presence of an evident crack pattern (Figure 7) and by its intrinsic vulnerability to out-of-plane actions. Indeed, flexural strength appears very limited for the lack of connections with the floors and the compromised interconnection with perpendicular walls. In addition, the risk

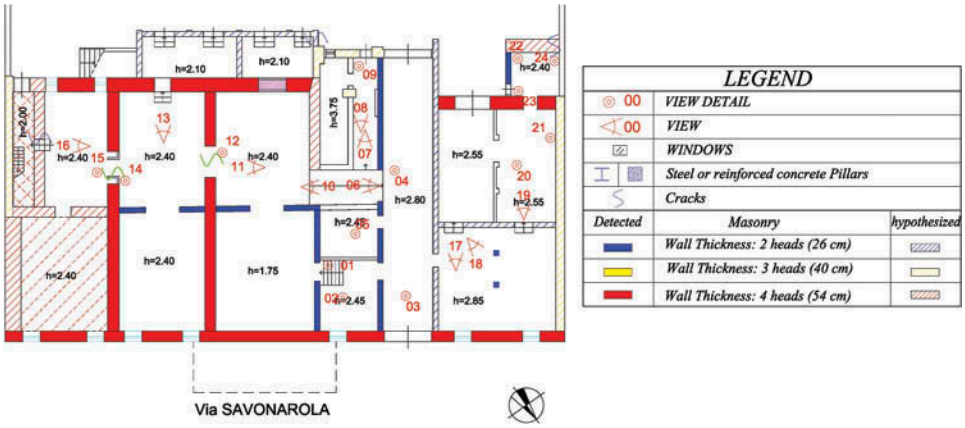

FIG. 5. Basement plan.

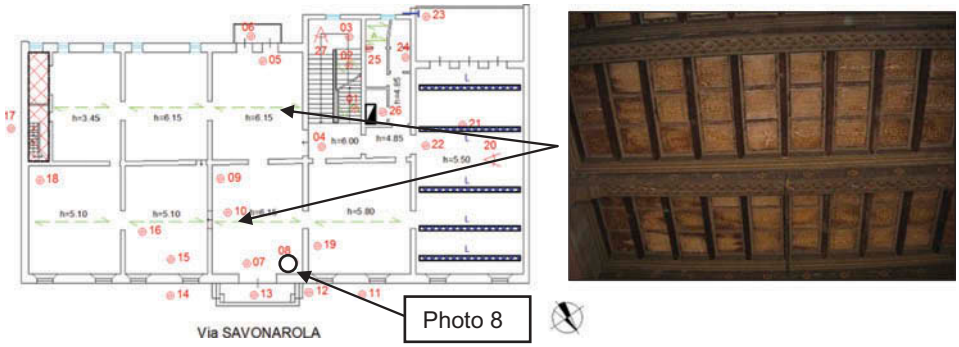

FIG. 6. Beam layout of the first floor (left) and photograph #8—details of the wooden floor (right).

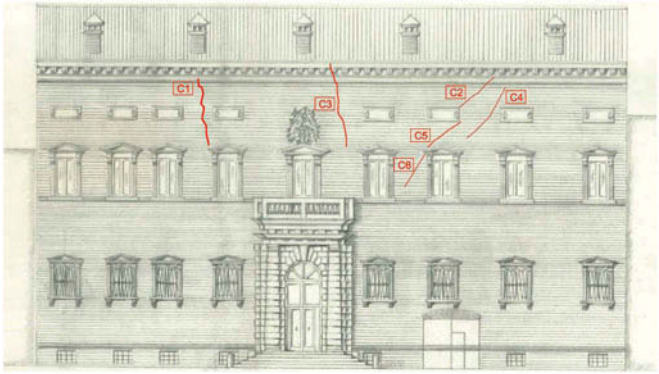

FIG. 7. Main facade with the surveyed crack pattern.

of a collapse on the main street makes its structural analysis extremely important and necessary. For these reasons, the present work is mainly concentrated on the structural behavior of this facade.

The crack opening on the facade overlooking the main road (Figure 7) varies from a few tenth of millimeters of the cracks C2, C4, C6, to 4–5 mm of the cracks C5 to 9–10 mm of the cracks C1 and C3. Three main cracks were decided to be investigated more deeply. The position of such cracks and the corresponding photos, along with the monitoring sensors, are also depicted in Figure 8 and Figure 9, respectively.

The cracks monitored by the sensors A and B are strictly related to the behavior of the main facade, whereas the crack monitored by the sensor C is not linked to the main facade but instead turns out to be relevant with reference to the general structural safety of the palace. These three cracks were monitored in the period February 22, 2012, to January 15, 2013. The corresponding results are well described in the Figure 10 together with the variation of the external temperature in the same period.

The jump in the monitored data, visible in Figure 10, is related to the seismic event that occurred in the region on the May 22, 2012. From the results depicted in the figure, it is possible to draw three main conclusions: 1) in the monitored period, the crack opening was not influenced by any founda-tion settlement, which means that it occurred previously and at the time of monitoring it was not in progress any longer; 2) the crack on the main facade is only influenced by the temperature variation during the year; this influence is clearly related to the fact that the crack monitored by the sensor A is the only one located externally and, thus, more influenced by the external climate; and 3) the jump in the crack opening occurring in the

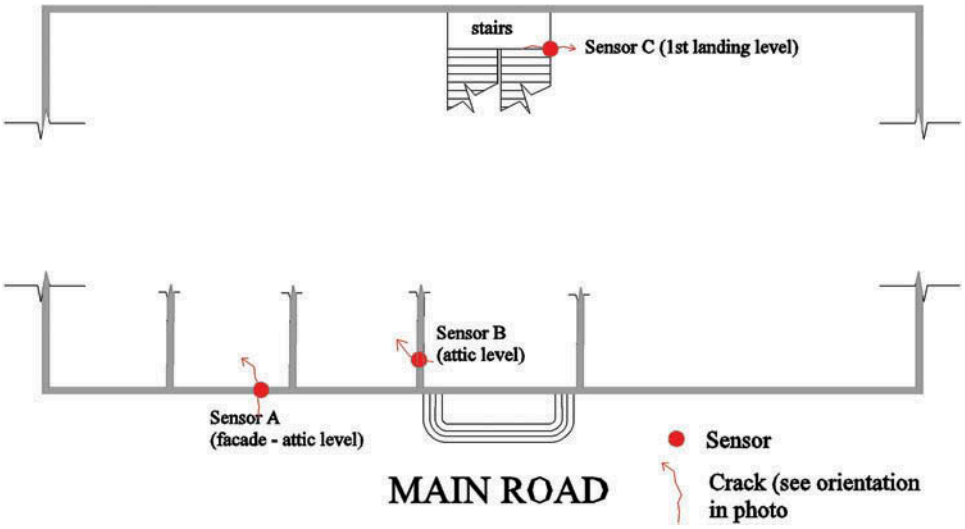

FIG. 8. Plan with the indication of the sensor positions.

FIG. 9. Photographs showing the orientation of the cracks and position of the sensors in Figure 8: sensor A (left), sensor B (center), sensor C (right).

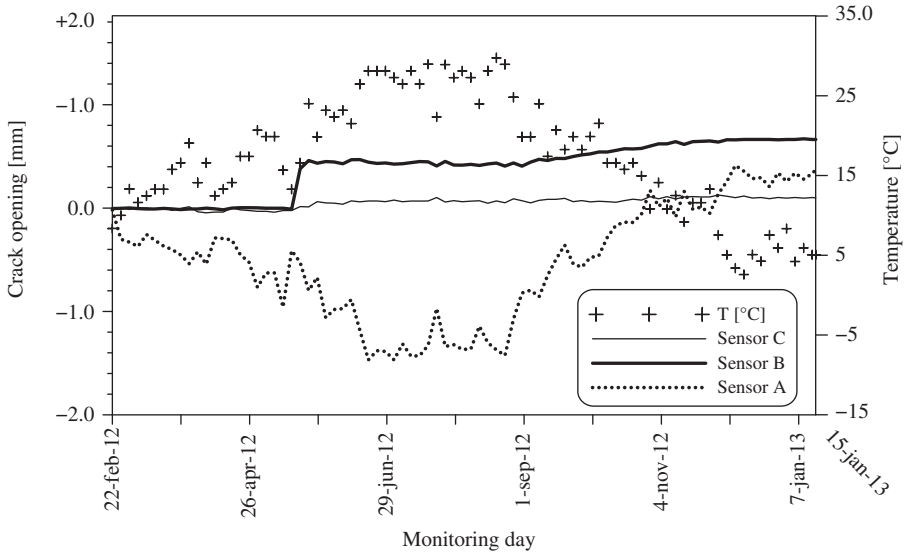

FIG. 10. Sensors monitored in the period from February 22, 2012, to January 15, 2013.

crack monitored by the sensor B allows to assess that cracks due to differential foundation settlements weaken the out-of-plane mechanical response of the masonry wall. Furthermore it is the authors' opinion that such a negative influence also occurs with reference to the in-plane strength of the masonry wall, even if it was not detected by the monitoring system because the out-of-plane mechanism was predominant in the context, as usually occurs in practice (Milani, Lourenço, and Tralli 2006b).

4. FINITE ELEMENT ANALYSES BY COMMERCIAL CODE

In order to deduce the actual differential settlements and to reproduce, at the same time, the surveyed crack pattern, two FE models are built with the aid of the commercial code Straus 7 (2004). First a three-dimensional (3D) of the entire Palace is built and discretized. The main facade is then modeled by a 2D discretization: in fact, such a part of the Palace deserves special attention and can be investigated separated from the remaining part of the Palace without introducing unacceptable errors. The survey underlined the particularly high structural vulnerability of the main facade, i.e., the crack pattern is mainly concentrated on such a portion. Furthermore, due to the intrinsic weakness of the wall-wall and wall-slab connections of the Palace, the 2D model is capable to reproduce the correct behavior of the facade without introducing inadmissible approximations and, at the same time, allowing repetitive analyses with a lower computational effort.

The main assumption of the models is that the differential settlement is due to a discontinuous mechanical behavior of the soil under the Palace. In the area of Ferrara, quick changes of the mechanical characteristics of the soil in the horizontal plane are quite usual. Furthermore, the low quality of the soil is very sensitive to changes of the applied load and to changes of the aquifer. In the present study, the discontinuity of the mechanical behavior of the soil was modeled as a change of the Winkler stiffness K. An inverse analysis would be neces-sary in order to establish the correct distribution of K in terms of values and location. Such an analysis is out of the scope of the present study. It must be also underlined that the issue is still open in the scientific literature, thus demonstrating the complexity of the problem. A parametric analysis was carried out on the basis of the structural survey and of the monitor-ing data. On the basis of such an analysis, it was clear that the discontinuity is capable to reproduce the surveyed crack pattern if two values of K are adopted (i.e., $K_1 = 3.8$ N/cm^3 and $K_2 = 8$ N/cm^3), and the distribution of K assumed as in Figure 11.

In the 3D model, the foundation under the portions of the Palace different from the main facade are modeled by Winkler springs with stiffness K equal to K_2. In order to compare the numerical results, it must be pointed out that the assumption of a Winkler-type foundation with variable stiffness K is also adopted in the homogenized FE model detailed in Section 5.

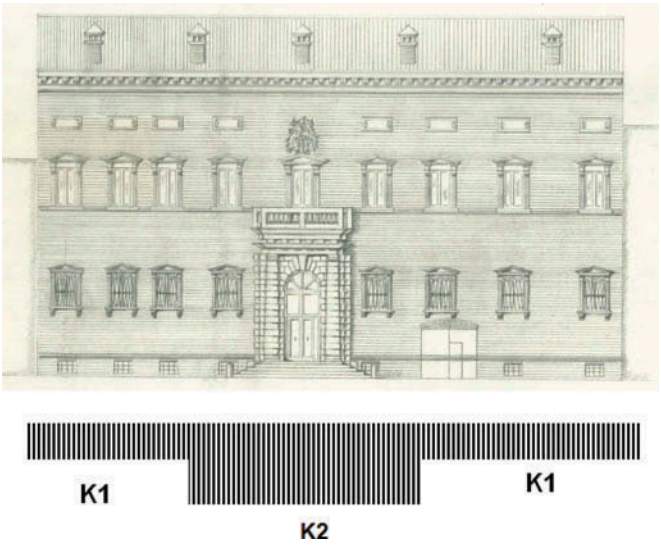

FIG. 11. Main facade with the adopted distribution of K in foundation.

4.1. Linear and Non-Linear Finite Element Analyses

A FE model of the entire building (Figure 12a), is built within the commercial code Straus 7.2 (Strand 7 2004) in order to have an insight into the stress state induced by the gravity loads and the foundation differential settlement on the Palace. Two hypotheses of increasing complexity are performed: the first model is linear elastic, and the second is an elastic-plastic approach for which a Mohr-Coulomb criterion is assumed at failure for masonry.

Eight-noded brick elements are used for masonry, assuming as vertical loads the masonry self-weight (the unit weight of the masonry was assumed equal to $\gamma = 18$ kN/m^3) plus dead and live loads on the floors. Floors are modeled by means of deformable four-noded plate and shell elements. Steel and timber beams sustaining wooded floors are meshed with standard two-noded Hermite elastic beam elements.

The second model is a typical elastic-plastic one, with a Morh-Coulomb failure criterion. Since it is not possible to use orthotropic materials with elastic-plastic behavior in the code, the elastic phase is fully governed by the Young and the shear moduli, assumed equal to 1290 MPa and 430 MPa respectively. This choice is perfectly in agreement with both Italian code requirements (Norme Tecniche per le Costruzioni [NTC] 2008) and the homogenized FE model (see results reported in the following Sections) and it is made on the basis of previous experimental experiences carried out by the authors on nearby coeval structures.

The soil under the structure is modeled by means of Winkler-type elastic springs as detailed in the previous section. The 3D models, whose discretizations and results are depicted from Figure 12 to Figure 16, were developed by assuming a foundation with variable mechanical characteristics under the Palace. Special attention was paid to the main facade: the main assumption was that its crack pattern was related to differential

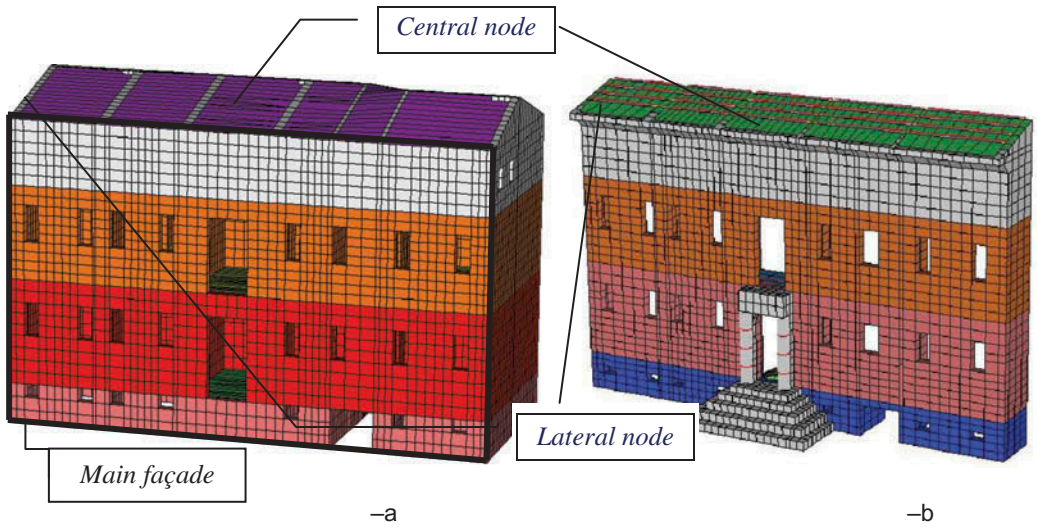

FIG. 12. Finite element model: (a) discretization of the entire building (8,958 solid elements, 851 plate and shell elements, 19,526 nodes); (b) discretization of the facade (2,776 solid elements, 590 plate and shell elements, 573 beam elements, 6,210 nodes). Different colors/shades of the elements indicate different floors.

settlements, thus, the numerical model was tested by assuming a discontinuous value of the main compressive mechanical prop-erties of the soil under the Palace, specifically by a discontinuity distribution of the Winkler stiffness K.

In order to limit the computational effort during elastic-plastic analyses, a partial FE model with very refined discretiza-tion comprising the facade and a portion of the perpendicular walls, as indicated in Figure 12-b, is also considered. The non-linear phase of the mechanical response of the masonry is modeled by the Mohr-Coulom failure criterion with cohesion equal to 0.1 MPa and friction angle 20°. No cut-off is consid-ered in tension. A perfect plastic behavior is assumed, within the classic hypotheses of the plasticity theory (associated flow rule and infinite ductility).

While the assumptions about the nonlinear behavior of the material are not fully realistic with reference to masonry, which, at failure, exhibits a orthotropic behavior (as demonstrated by many authors, such as Milani, Lourenço, and Tralli 2006a), softening after the peak load (Lourenço and Rots 1997; Mallardo 2009; Milani 2011; Milani and Tralli 2012,) and non-associativity under shear loads (Ferris and Tin-Loi 2001; Orduna and Lourenço 2005; Gilbert, Casapulla, and Ahmed 2006), the proposed approach is more detailed with respect to the standard linear elasticity procedure and it allows a rough preliminary estimation of the portions of the facade undergoing inelastic deformation, that is, crack openings. In addition, it is worth noting that available commercial FE codes, as the one used in this case, can rarely be used for a realistic anal-ysis of masonry beyond the elastic limit, because incapable of properly reproducing—as still under research investigation—all specific properties exhibited by masonry. It must be underlined that the post-peak behavior of the crack has little influence on the global response of the masonry structure as energetically negligible and therefore no special attention was paid to the use of special software (e.g., Atena FE code [Cervenka, Jendele, and Cervenka 2007]) in order to include such an aspect.

The use of geometrically simplified models (the facade and a portion of the perpendicular walls) when dealing with the elastic-plastic approach allows a less demanding computational effort, at the same time providing interesting information beyond the elastic limit, as for instance the portions of the facade undergoing inelastic deformation, once again under the hypothesis of a foundation supported by springs with different elastic stiffness.

4.2. Numerical Results

In order to validate the results obtained with the linear elas-tic analysis, the elastic-plastic simulations have been repeated on the whole structure (depicted in Figure 12a), obviously with a very demanding computational effort that cannot be han-dled within a recursive strategy based on the iterative change of the Winkler spring stiffness at the base. Some of the most meaningful results obtained with the linear elastic analysis are represented in Figure 13, Figure 14, and Figure 15. In particular, a gray-scale contour plot representing the vertical displace-ments of the structures under vertical loads (gravity, dead, and live loads) and the deformed shape of the facade are shown in Figure 13, whereas the direction of the maximum principal stresses are depicted in Figure 14. The maximum principal stresses directions and the intensity of the stresses exceeding masonry tensile strength exhibit a promising match with the existing crack directions (Figure 15), preliminarily confirming that the state of damage may be ascribed to a differential settlement in correspondence of the foundation level. Vertical displacements are less evident in the central zone (near 3 mm) and much larger in the lateral zones (> 6 mm), as shown in Figure 13.

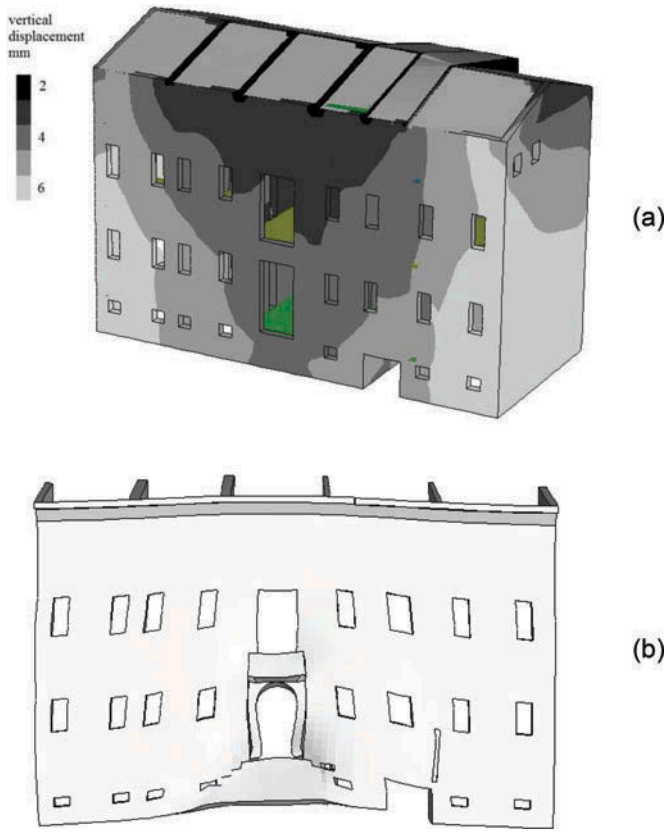

FIG. 13. Three-dimensional models: (a) grey-scale map representing the vertical displacements of the entire building under gravity, dead and live loads; (b) deformed shape of the facade.

Simple geometrical considerations carried out on portions of the facade assumed as rigid blocks allow to conclude that such displacements near the base may result into cracks open-ing at the last floor larger than 10 mm, again a result in good agreement with the actual crack pattern.

The results, obtained by means of the elastic-plastic analysis carried out on the isolated facade (the discretization is shown in Figure 12b), are summarized in Figure 16, where the displacements were recorded in correspondence of two nodes at the last floor level, the first located in the lateral zone of the facade, the second near the center (Figure 12 shows the exact position of the nodes). Two curves are compared, the first obtained with the elastic-plastic approach performed on the isolated facade, the second resulting from the elastic-plastic analyses carried out on the whole building.

As can be noted, a similar trend of the displacement plots is obtained, with a comparable final amount of vertical displacements, but with a more marked non-linearity of the global model, probably due to a relevant contribution of out-of-plane deformation not easily reproducible with the partial model.

It is worthy to underline that an incremental scheme is adopted within the proposed elastic-plastic approach: the software allows the gravity loads to be incremented from zero to their actual value by means of 20% steps; internal substeps are

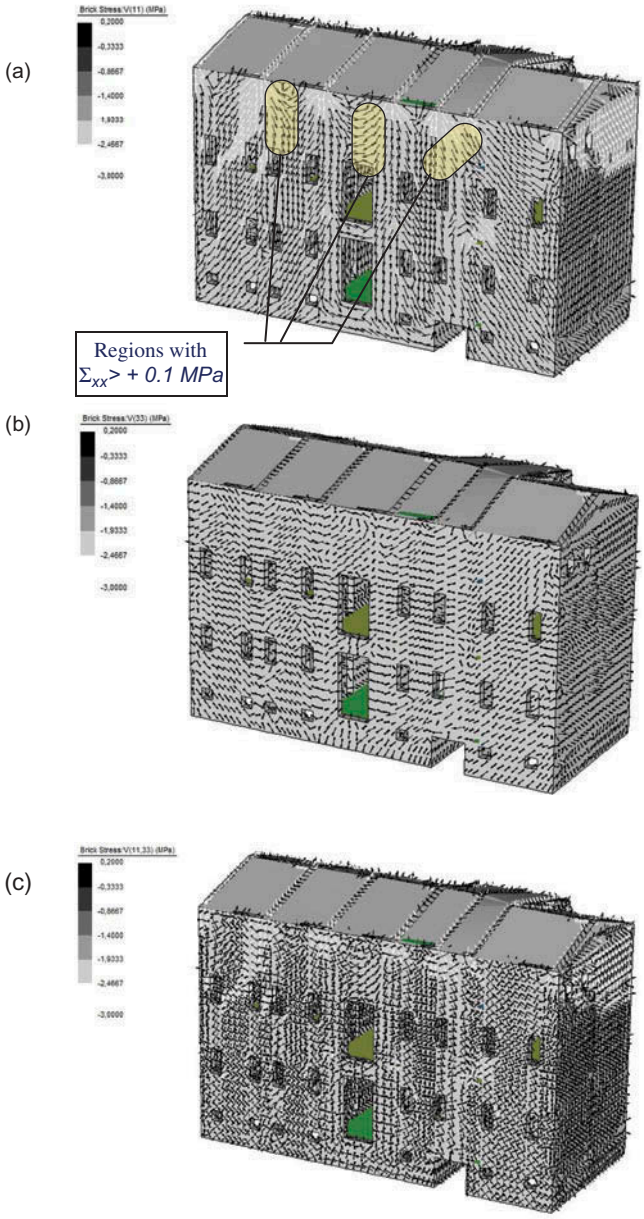

FIG. 14. Three-dimensional models: (a) maximum principal stress directions, (b) minimum principal stress directions, (c) combined maximum and minimum stress directions.

carried out in order to obtain the convergence. As a matter of fact the historical analysis of the palace may admit the possibility that it might have been built first as three *casseri* and then the fourth *cassero* added adjacent to it. In order to simulate such a construction a more rigorous so called FE *staged construction analysis* would have had to be tested: staged construction is a static modeling strategy which enables the definition of a sequence of construction stages in which structural systems and load patterns are added or removed, and time-dependent behaviors are evaluated. The simulation is rather complicated, it is allowed in very few sophisticated FE software programs, and it

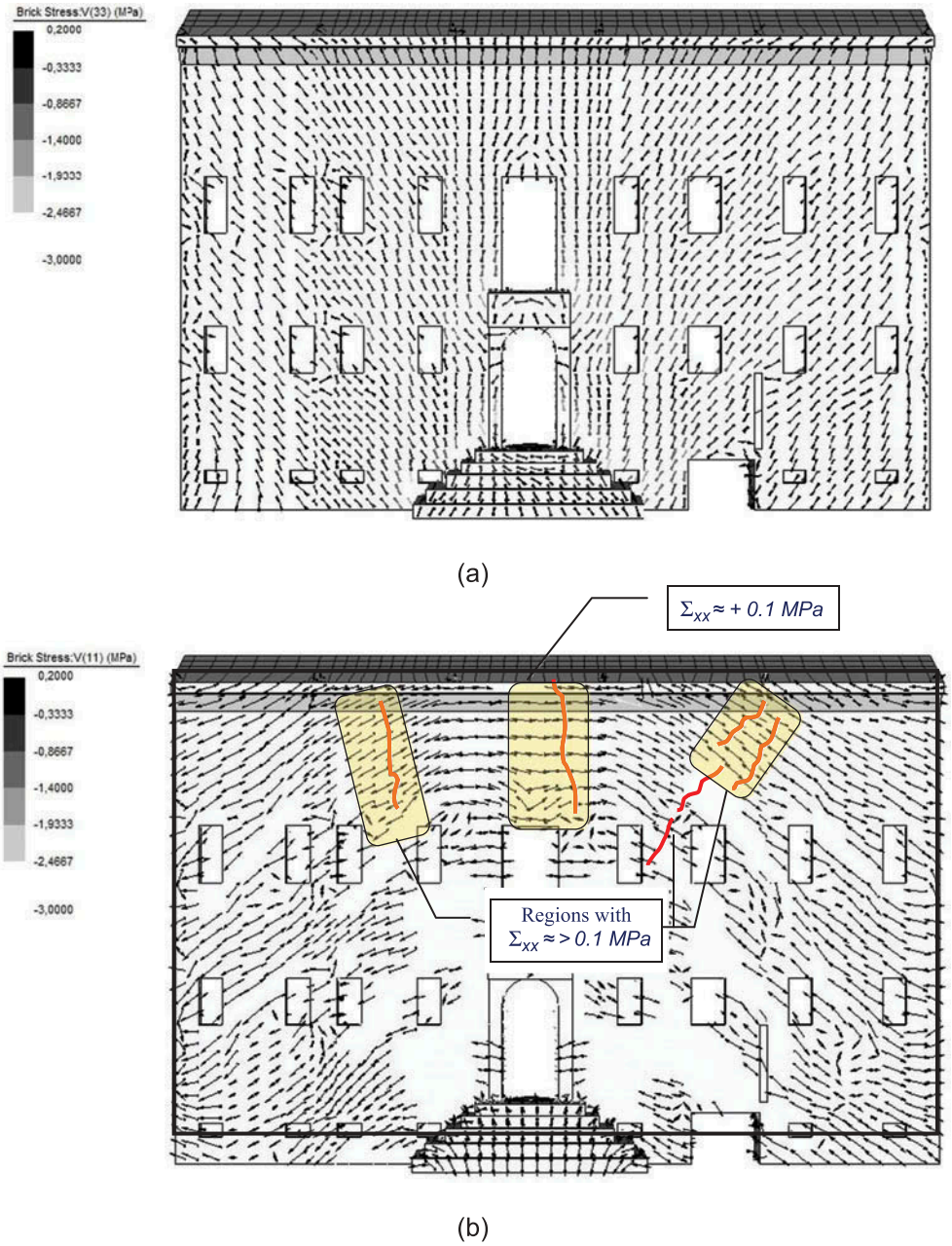

FIG. 15. Direction of the principal stresses, partial model: (a) minimum principal stress directions, (b) maximum principal stress directions with comparison of position of actual cracks and those provided by the numerical model.

is still under progress; for this reason and due to the fact that the adopted simplification was able to reproduce realistic results, it was not implemented.

5. NUMERICAL HOMOGENIZED FINITE ELEMENT ANALYSIS

A complex but very detailed FE non-linear analysis is here carried out by means of the homogenized FE approach firstly presented in Milani (2011).

In particular, a discretized model where masonry is represented by means of rigid triangular elements interconnected by non-linear shear and normal springs representing homogenized masonry is used. The approach has been already tested on a variety of different medium and large scale structural problems in Milani (2011) and Acito and Milani (2012), including large scale 3D structures subjected to differential displacements at the base. The software is fully non-commercial and it is suitable for the analysis of complex masonry structures in the non-linear range, that is, to take into account the anisotropy in

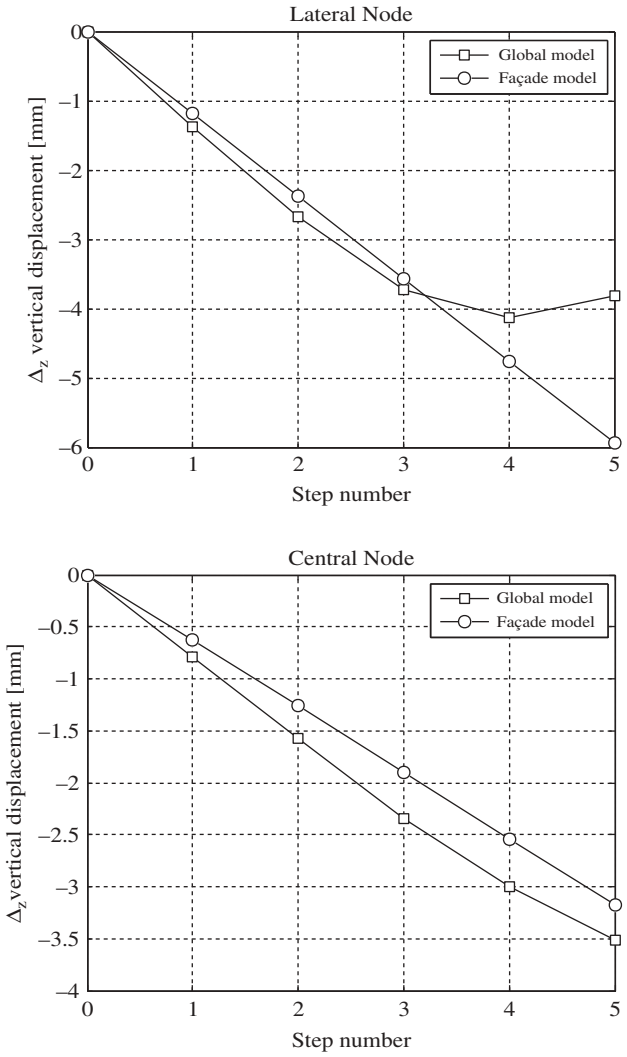

FIG. 16. Comparison between vertical displacements provided by the elastic-plastic global and partial models. Top: lateral node, last floor level. Bottom: central node, last floor level.

the linear and non-linear range and the softening behavior in tension.

The approach is composed of two steps. In the first step, masonry is substituted with a fictitious homogeneous material by means of the solution of a boundary value homogenization problem in the non-linear range on a suitable REV, which generates the whole structure by repetition. The homogenization proposed pertains to running bond non-strengthened masonry, regarded as an assemblage of bricks interacting through interfaces (mortar joints). Bricks are supposed infinitely resistant, whereas a Mohr Coulomb failure criterion with tension cut-off and compressive limited strength is adopted for the joints. Then, the obtained non-linear homogenized behavior is implemented at a structural level, assuming the non-linear mechanical behavior deduced from homogenization for the interfaces between contiguous triangles. A reliable quadratic programming approach is adopted to solve the incremental problem, allowing for a robust handling of the interfaces softening behavior.

In what follows, the basic theoretical and numerical aspects of the procedure adopted are briefly reviewed.

5.1. Meso Scale Approach: Heterogeneous Model

In the heterogeneous model, the REV is meshed through 24 three-noded elastic triangular elements interconnected by non-linear interfaces (internal brick-brick interfaces and mortar joints, as shown in Figure 17).

With such a discretization, a homogenized incremental boundary value problem is solved to numerically estimate the average non-linear behavior of the REV under different in-plane load conditions. Full details of the procedure may be found in Milani (2011) and Milani and Tralli (2012), whom the reader is referred to for further details.

For a mortar interface, the elastic domain is, in the most general case, bounded by a composite yield surface that includes tension, shear and compression failure with softening. A multi-surface plasticity model is adopted, with softening in both tension and compression.

In order to model the failure of the joint, a classical Mohr–Coulomb type strength criterion is used with eventually a tension cut-off (Figure 18). The parameters f_t and f_c are, respectively, the tensile and compressive Mode-I strength of the mortar or mortar–brick interfaces, c is the cohesion, Φ is the friction angle, and Ψ is the angle which defines the linear compression cap.

For the tension mode, exponential softening on the tensile strength is assumed according to the mode I experiments conducted by many authors. The yield function reads:

$$f_1(\boldsymbol{\sigma}, \kappa_1) = \sigma - f_t(\kappa_1) \tag{1}$$

where the yield value $f_t(\kappa_1)$ deteriorates in agreement with the following formula:

$$f_t(\kappa_1) = f_{t0} e^{-\frac{f_{t0}}{G_f^I}\kappa_1} \tag{2}$$

where f_{t0} is the initial joint tensile strength and G_f^I is the mode I fracture energy. An associated flow rule is assumed here.

When dealing with the shear mode, a Mohr-Coulomb yield function is adopted:

$$f_2(\boldsymbol{\sigma}, \kappa_2) = |\tau| + \sigma \tan\phi(\kappa_2) - c(\kappa_2) \tag{3}$$

where $|\tau| = \sqrt{\tau_1^2 + \tau_2^2}$ and the yield values c and $\tan\phi$ are ruled by the following formulas:

$$c(\kappa_2) = c_0 e^{-\frac{c_0}{G_f^{II}}\kappa_2}$$

$$\tan\phi = \tan\phi_0 + (\tan\phi_r - \tan\phi_0)(c_0 - c)/c_0 \tag{4}$$

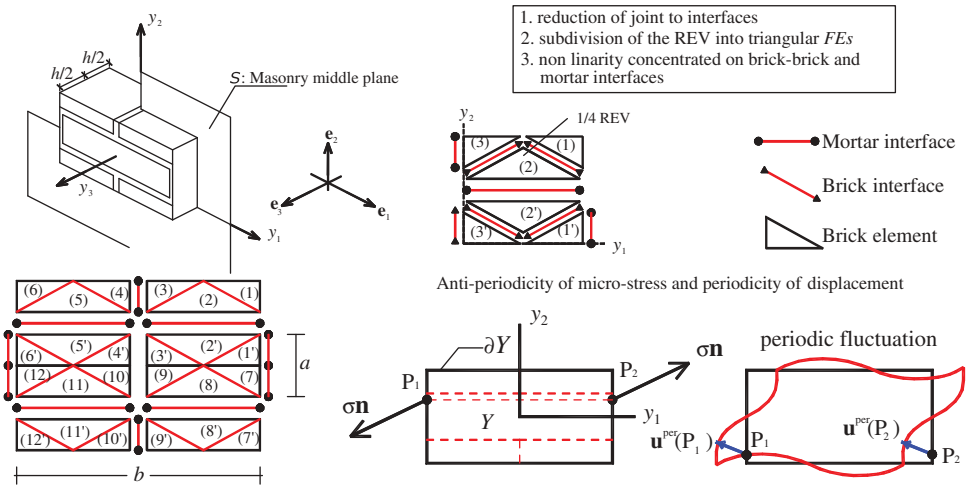

FIG. 17. The micro-mechanical model proposed. Subdivision of the representative element of volume (REV) into 24 triangular elements (and 1/4 into six elements) and anti-periodicity of the micro-stress field.

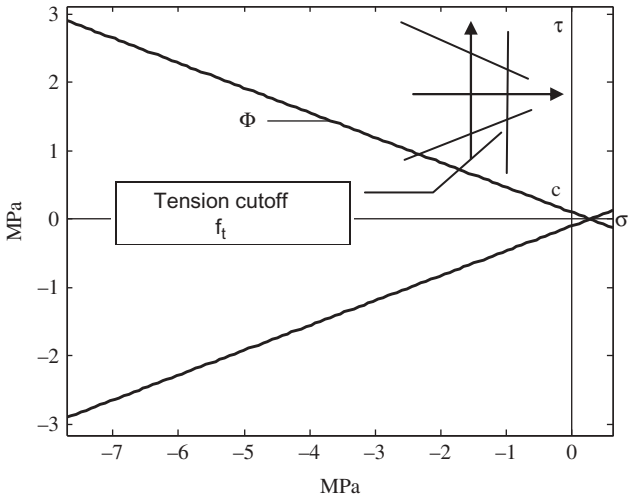

FIG. 18. Linearized failure surfaces adopted for mortar in the softening model with rigid elements and interfaces.

being c_0 and $\tan\phi_0$ the initial cohesion and friction angle, G_f^{II} is the mode II fracture energy and $\tan\phi_r$ is the residual fric-tion angle, hereafter kept always equal to 75% of the initial one. A non-associated flow rule is assumed here, with $g_2 = |\tau|$.

For the sake of simplicity, in the present model the inelastic behavior in compression is excluded from the numerical analyses. In Lourenço and Rots (1997), a more sophisticated model was presented, with an inelastic behavior in compression ruled by a three function model reproducing the typical initial ductility of masonry in compression, followed by crushing.

The present final homogenized model representing masonry with brick-brick interfaces and joints is orthotropic; the final adopted values can be easily deduced from the uniaxial response of the homogenized material represented in Figure 19.Itiswor-thy to underline that the final Young's modulus in the vertical direction is 1) close to the value used in the FE model described in the previous section, 2) approximately equal to the value suggested by the Italian Technical Code (the NTC [2008] and the related Circolare 617 [2009]).

5.2. Numerical Simulations at a Cell Level

This section provides an insight into the inelastic behavior provided by the non-linear homogenization model proposed in the paper. To this aim, we consider the typical REV of the palace constituted by bricks of dimensions 210 × 52 × 100 mm^3. Elastic and inelastic material properties are sum-marized in Table 1. Values adopted for cohesion and masonry elastic moduli are taken in agreement with Table C8A.2.1 in Circolare 617 (2009), with a knowledge level LC (confidence factor FC = 1.35) and with a correction coefficient equal to 1.5, in agreement with Table C8A.2.2 Circolare 617. It is worth noting that the data assumed are in agreement with those adopted within the isotropic commercial code model. A friction angle equal to 20° is assumed, again in agreement with the Italian code.

Two different values of the fracture energy G_I are assumed to test the inelastic behavior of the REV, the first corresponding realistically to existing masonry (Case A), the second approximating an almost perfect plastic behavior in tension (Case B). The behavior in uniaxial tension is depicted in Figure 19 for both horizontal (a) and vertical (b) tension. The anisotropy of the homogenized model is particularly evident and is mainly due to the contribution in horizontal tension of the bed joint, which fails in shear (REV deformed shape is represented in Figure 19c for the sake of completeness with the indication of the typology of failure registered by the code).

It has been proven, Milani (2011), that with very refined discretizations of the REVs, negligible differences are found in both the peak and post-peak behavior, as well as in the failure mechanism. Indeed, being the non-linearity mainly

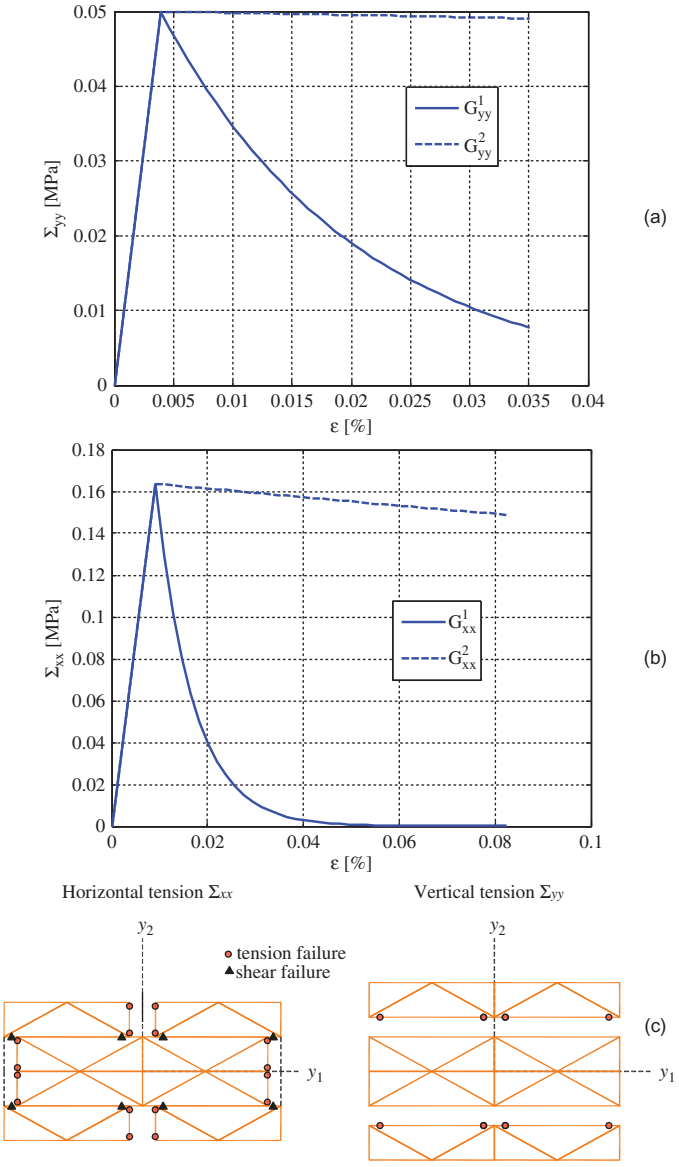

FIG. 19. (a, b) Uniaxial response of the homogenization model along vertical (a) and horizontal (b) tension for two values of fracture energy. (c) Representative element of volume (REV) deformed shape at collapse with indication of interface damage in horizontal tension (left) and vertical tension (right).

concentrated in joints reduced to interfaces, it can be noticed that for both vertical and horizontal stretching – as well as for shear - the response of the coarse mesh is expected to be the same of that obtained with a refined discretization.

Compression behavior is less important when dealing with the detection of crack patterns induced by foundation settlement. For this reason and for the sake of simplicity, in what follows non-linearity in compression is excluded.

Finally, in Figure 20, the pure shear behavior of the REV is represented at three increasing vertical values of pre-compression. As expected, both peak strength and ductility increase; once again, the output provided by the numerical model is reasonably in agreement with available experimental data and existing numerical models.

5.3. Homogenized Step-By-Step Non-Linear Analyses

The present analyses require a structural implementation with discretization of masonry with six-noded rigid infinitely resistant wedge shaped elements (Kawai 1978). In this way, all deformation is concentrated exclusively on interfaces (modeled assuming a homogenized orthotropic material derived with the procedure previously discussed, see also Milani et al. 2008), thus requiring a very limited number of optimization variables to be performed. Kinematic variables for each element are represented by three centroid velocities (u^E_x, u^E_y, u^E_z) and three rotations around centroid G (Φ^E_x, Φ^E_y, Φ^E_z).

To estimate plastic deformation, it is necessary to evaluate the jump of velocities or displacements (for respectively limit and non-linear static analysis) on interfaces. To do this, it is simply necessary to evaluate the displacement of a point P of the interface as belonging alternatively to M and N, assuming that M and N are two wedge elements defining the interface. After trivial algebra, the jump can be evaluated in the global coordinates system as:

$$[\mathbf{U}(P)] = \mathbf{U}^G_M - \mathbf{U}^G_N + \mathbf{R}_M (P - G_M) - \mathbf{R}_N (P - G_N) \qquad (5)$$

where $[\mathbf{U}(P)]$ is the displacement jump in P, $\mathbf{U}^G_I$ is the displacement vector of element I centroid (point G_I) and $\mathbf{R}_I$ is a 3×3 rotation matrix for element I containing rotations around centroid.

After defining a local frame of reference $\mathbf{e}_1$-$\mathbf{e}_2$-$\mathbf{e}_3$ with $\mathbf{e}_3$ normal to the interface and $\mathbf{e}_1$-$\mathbf{e}_2$ on the interface plane and denoting with $\mathbf{R_e}$ the rotation matrix with respect to the global coordinate system, jump of displacements (5) may be written in the local system as $\left[\tilde{\mathbf{U}}(P)\right] = \mathbf{R_e}[\mathbf{U}(P)]$ where the superscript $\sim$ indicates quantities evaluated in the local system.

To solve the non-linear structural analysis problem, under some general hypotheses holding for materials exhibiting an elastic-plastic behavior (for instance, the plasticity condition is piecewise-linearized with r linearly elastic-plastic interacting planes in the space of superimposed stress and strain components, the unloading of yielded stress-points does not occur and the continuum is discretized into finite elements) the incremental problem can be solved using the following quadratic programming formulation (Grierson et al. 1979, Capurso & Maier 1966):

$$\begin{cases} \max \left\{ -\frac{1}{2}\left(\boldsymbol{\lambda}^E\right)^T \mathbf{H}^E \boldsymbol{\lambda}^E + \left(\boldsymbol{\lambda}^E\right)^T \left(\mathbf{N}^E\right)^T \mathbf{D}^E \boldsymbol{\varepsilon}^E \right. \\ \qquad \textit{subject to} : \boldsymbol{\lambda}^E \geq \mathbf{0} \\ \qquad \boldsymbol{\varepsilon}^E_t = \boldsymbol{\varepsilon}^E + \boldsymbol{\varepsilon}^E_{pl} \\ \qquad \boldsymbol{\sigma}^E = \mathbf{D}^E \boldsymbol{\varepsilon}^E_{pl} \end{cases} \qquad (6)$$

TABLE 1
Mechanical properties adopted for the constituent materials

	Joint	Brick-brick interface	Units of measure	
E	400	1600	[MPa]	Young Modulus
G	170	670	[MPa]	Shear Modulus
c	0.05	—	[MPa]	Cohesion
f_t	0.05	—	[MPa]	Tensile strength
Φ	20	—	[°]	Friction angle
G_f^I	0.001 (Case A) 0.1 (Case B)	—	[N/mm]	Mode I fracture energy
G_f^{II}	0.002 (Case A) 0.2 (Case B)	—	[N/mm]	Mode II fracture energy

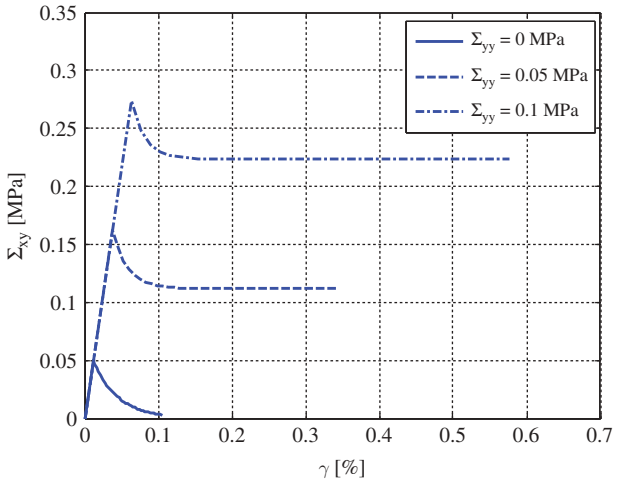

FIG. 20. Shear behavior of the representative element of volume (REV) at three levels of increasing pre-compression.

Where $\mathbf{D}^E$ is the assembled elastic stiffness matrix, $\boldsymbol{\varepsilon}^E(\boldsymbol{\varepsilon}_{pl}^E)$ is the assembled elastic (plastic) part of the total strain vector $\boldsymbol{\varepsilon}_t^E$, $\mathbf{N}^E$ is the shape functions matrix of the used finite element, $\boldsymbol{\lambda}^E$ is the plastic multiplier vector, $\mathbf{H}^E$ is the hardening matrix and $\boldsymbol{\sigma}^E$ the assembled stress vector.

Within the FE model adopted, it can be shown that problem (6) may be re-written for the problem at hand (rigid elements with elastic-plastic interfaces) as follows:

$$\begin{cases} \min \left\{ \frac{1}{2} \left[\left(\boldsymbol{\lambda}^+ - \boldsymbol{\lambda}^-\right)^T \mathbf{K}_{ep} \left(\boldsymbol{\lambda}^+ - \boldsymbol{\lambda}^-\right) + \mathbf{U}_{el}^T \mathbf{K}_{el} \mathbf{U}_{el} \right] - \mathbf{F}^T \mathbf{U}_{el} \right. \\ \qquad \textit{subject to} : \boldsymbol{\lambda}^+ \geq \mathbf{0}\ \boldsymbol{\lambda}^- \geq \mathbf{0} \end{cases} \tag{7}$$

Assuming that the structural model has n_{in} interfaces and n_{el} elements, symbols in equation (7) have the following meaning:

1. $\mathbf{K}_{el}$ is a $6n_{el} \times 6n_{el}$ assembled matrix, collecting elastic stiffness of each interface.
2. $\boldsymbol{\lambda}^+$ and $\boldsymbol{\lambda}^-$ are two $10n_{in}$ vectors of plastic multipliers, collecting plastic multipliers of each nonlinear spring (e.g. flexion, shear, etc.).
3. $\mathbf{K}_{ep}$ is a $10n_{in} \times 10n_{in}$ assembled matrix built from diagonal matrices of hardening moduli of the interfaces.
4. $\mathbf{U}_{el}$ is a $6n_{el}$ vector collecting the displacements and rotations of the elements.
5. $\mathbf{F}$ is a $6n_{el}$ vector of external loads (forces and moments) applied on element centroids.

Typically, the independent variable vector is represented by element displacements $\mathbf{U}_{el}$ and plastic multiplier vectors $\boldsymbol{\lambda}^+$ and $\boldsymbol{\lambda}^-$.

To deal with mortar joints softening, the behavior of the springs is approximated using a stepped function and Quadratic Programming (Milani and Tralli 2012).

5.4. Numerical Results

The numerical model previously described and already presented in Milani (2011) without translational elastic springs representing soil stiffness, has been here generalized in presence of a Winkler model.

Before presenting the results, it is worth underlining that, in the model, the following hypothesis are implicitly assumed:

- The mechanical properties of the materials are derived fitting as close as possible experimental data available for the masonry under consideration, through homogenization theory. The inelastic behavior of the masonry, see Figure 19, realistically reproduce the actual proper-ties of the masonry under consideration, also reflecting the expected orthotropy ratio for the texture considered and the actual disposition and geometry of the bricks. However, the model is unable to reproduce in detail the actual cracks typically zigzagging between con-tiguous bricks. Only a general trend of 1) the position,
  2) the direction and 3) the width of the cracks may be obtained.

- The structural model relies on a discretization with rigid triangular elements and interfaces. Cracks propagation, if any, is therefore constrained to run between contiguous elements and therefore results intrinsically mesh dependent. A re-meshing procedure within a non-linear programming approach may be attempted to eliminate this critical drawback, as already done in limit analysis by Milani and Lourenço (2009) using sequential linear programming.
- A simplified evaluation of crack pattern opening to compare with the sophisticated FE nonlinear results is also proposed. The simplified mechanical model considered is sketched in Figure 21. It consists of a rigid block representing the left hand side of the facade that is supposed free to rotate when subjected to an increase of the dead loads from zero to their actual value around a hinge located in correspondence of the base, on point A. Base Winkler springs oppose to the rotation with a stabilizing bending moment equal to $M_{K1}(\vartheta) = \int_0^L (K_1 \vartheta x)\, x dx = K_1 \frac{L^3}{3}\vartheta$, where ϑ is the rotation of the rigid block and L its length, as indicated in Figure 21. The bending moment of the vertical masonry section where the crack propagates is $M_M(\vartheta)$ and may be easily evaluated from homogenization the-ory, see previous Sections, when the tensile strength of the masonry material f_{tx} is known. Typically, in absence of horizontal pre-compression and assum-ing an infinite compressive strength for the sake of simplicity, the rotation-moment relationship exhibits marked non-linearity with softening. In order to pass from curvatures to rotations, an energy equivalence between an elastic cantilever beam with length equal to L and a rigid beam with concentrated elastic rota-tional spring is used. Both structures are assumed to be subjected to a distributed load representing dead loads. Rotational equilibrium conditions of the rigid block require that:

$$PL' = M_{K1}(\vartheta) + M_M(\vartheta) \tag{8}$$

where P is the total amount of vertical loads and L' is the horizontal distance of its point of application from point A. When the vertical loads are incremented from zero to their actual value, as it occurs in the simplified procedure adopted in this study, equation (8) is non-linear in ϑ (due to $M_M(\vartheta)$) and ϑ is evaluated resorting to consolidated recursive computations. Vertical displacement of the top corner, to compare with Straus results, is equal to ϑH, whereas crack width, to compare with homogenized FE computations, is ϑL.

For the example under consideration, the FE discretization shown in Figure 22a on the deformed shape of the structure obtained at the end of the non-linear static analysis is adopted. In Figure 22b crack width opening (the crack under consideration is highlighted in Figure 22a) versus gravity loads multiplier is represented.

As can be seen, the node monitored for the comparison is positioned immediately under the roof and near the center of the facade. The crack width amount (approximately 10 mm) found in the numerical analysis, as well as its direction seem to well approximate the results of the survey. In particular, the direction of the crack corresponds roughly to the observed one, which appears almost vertical. The agreement between the homogenized FE approach and the rigid block response (both assuming the exact moment-rotation diagram in Figure 21b or its multi-linear approximation) is worth noting.

In addition, from an overall analysis of the deformed shape at the end of the simulations, Figure 22a, it can be noted that the overall crack pattern exhibited by the facade is reproduced with a quite satisfactory accuracy, meaning that the combined analytical numerical approach proposed may provide rather accurate predictions of the state of degradation of the building. In order to predict the future evolution of the cracks, it may be interesting to run the numerical model in the presence of a linear decrease of the stiffness values of lateral Winkler springs K1, from their present value to 1/4. Such a situation appears the most unfavorable one, such that may occur in the presence of a soil load-bearing capacity vanishing under the foundation of the facade in lateral zones.

Results are reported in Figure 23, where the new deformed shape of the facade at the end of the simulations and the crack width of the same node previously considered are depicted. Obviously the pre-existing cracks spread considerably from the upper part to the lower floors levels. In addition, new cracks appear near the triumphal arch and immediately over the foundation, in correspondence of the change of stiffness of the springs.

6. NUMERICAL: EXPERIMENTAL RESULTS COMPARISON AND DISCUSSION

In order to carry out a fruitful comparison of the numerical results obtained by the two FE models described in the previous sections, the differential settlements along an horizontal line close to the foundation of the Palace were measured with a high precision auto level (Leica NA 700 Series, NA730 model). Such measurements (in millimeters) are depicted in Figure 24. Points are kept with a horizontal step equal to 150 cm.

The zero point, i.e. the node exhibiting zero vertical displacement, is considered the portal threshold, which exhibits a quite flat shape. In order to compare such results with the numerical data it is therefore necessary to add to such measured values the actual vertical displacement of the portal, which is roughly

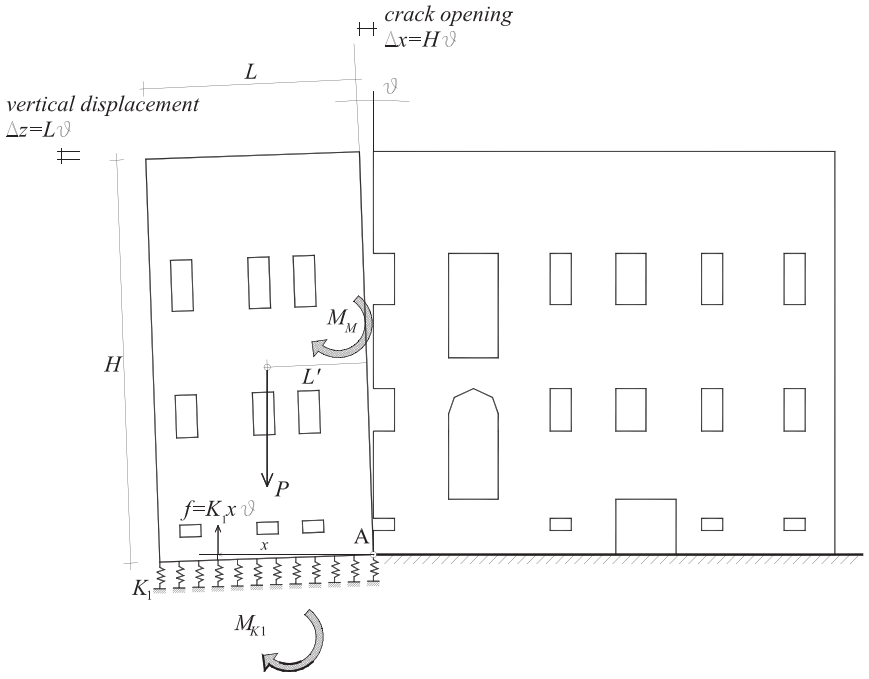

(a)

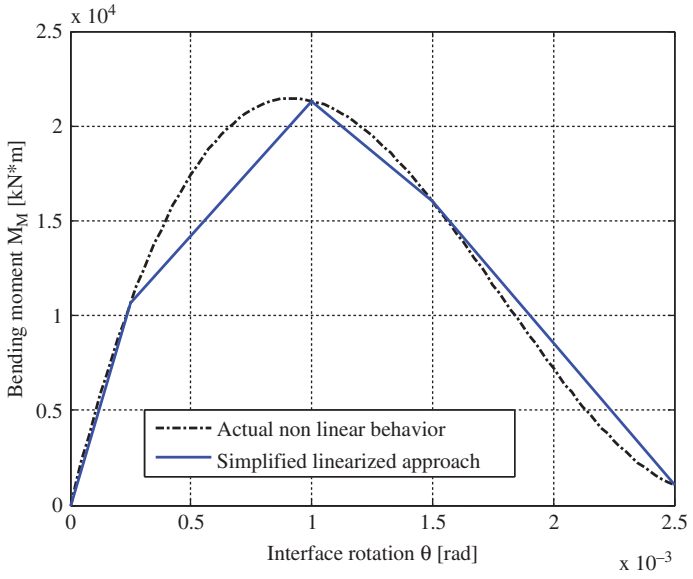

(b)

FIG. 21. (a) Simplified mechanical model adopted to compare with finite element predictions; (b) moment curvature behavior assumed in the model and its multi-linear approximation.

assumed equal to 2 mm, in agreement with all displacements provided by the numerical models (both global and partial).

The comparison between foundation settlement profiles, provided by the different numerical models, and experimental data is finally provided in Figure 25, where a good agreement among the different numerical models and between experimental evidences and numerical simulations is clearly visible.

A detailed analysis of the results obtained by means of the comprehensive integrated study carried out allows to conclude that the crack pattern of the facade is certainly a consequence of a differential foundation settlement induced by a not uniform stiffness of the soil under the foundation of the building (softer on the lateral, right and left, parts) and partially by the completion of the facade with the transformation of the service wing into a further cassero.

The monitoring activity carried out by the authors on the main cracks of the facade and on the perpendicular walls lets to think that cracks are stable, i.e. the state of damage is not getting worse. The recent seismic event caused a 0.5 mm additional opening of the crack on a wall perpendicular to the facade

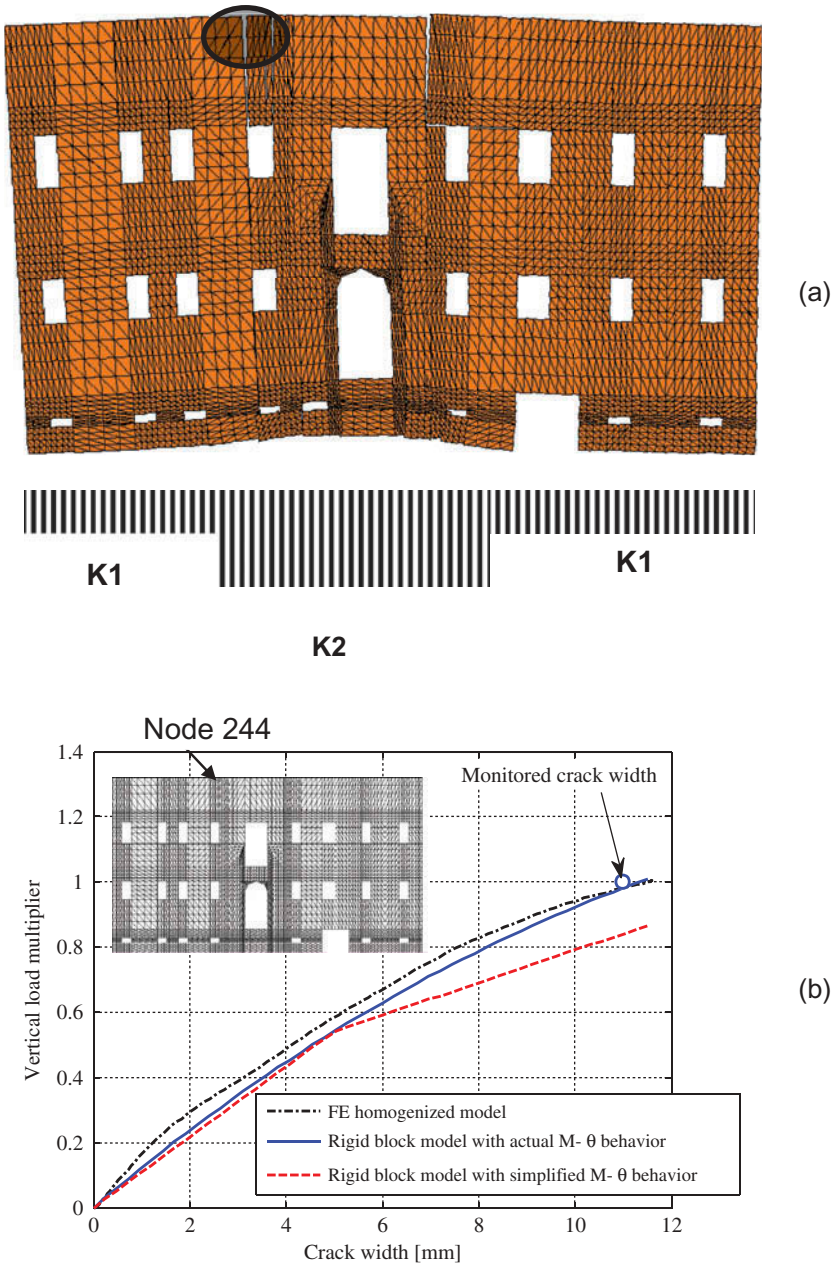

FIG. 22. (a) Deformed shape of the facade at the end of the non-linear simulations (6880 triangular elements); (b) crack width versus vertical load multiplier.

and monitored by sensor B, whereas other cracks did not exhibit perceptible movements. Therefore, it is straightforward to state that the out-of-plane movement of the facade has to be further investigated and a prediction of the facade's load bearing capacity under seismic loads should be taken in the due consideration in order to assess its vulnerability. It is worth emphasizing that the facade, when subjected to horizontal loads in its present situation—with the existing crack pattern, is certainly expected to be much more vulnerable than it would be in its undamaged configuration, since cracks represent preferential areas of weakness where flexural yield lines propagate.

In this context, the prediction of the formation of the crack and of its evolution is of fundamental importance for a seismic evaluation. The integrated use of the data provided by the installed monitoring system and the FE simulations, carried out by using both commercial codes and sophisticated nonstandard homogenization procedures, allows to have a prediction of the facade behavior and provides interesting information for specialized and targeted interventions of rehabilitation, also in the light of a seismic upgrading of the structure.

A standard elastic-plastic approach based on the use of isotropic materials may not represent with sufficient care the actual behavior of the facade; however, if it is coupled with a sophisticated analysis with isotropic materials derived from rigorous homogenization and softening behavior, it can be sufficiently predictive. That is even truer if the few material

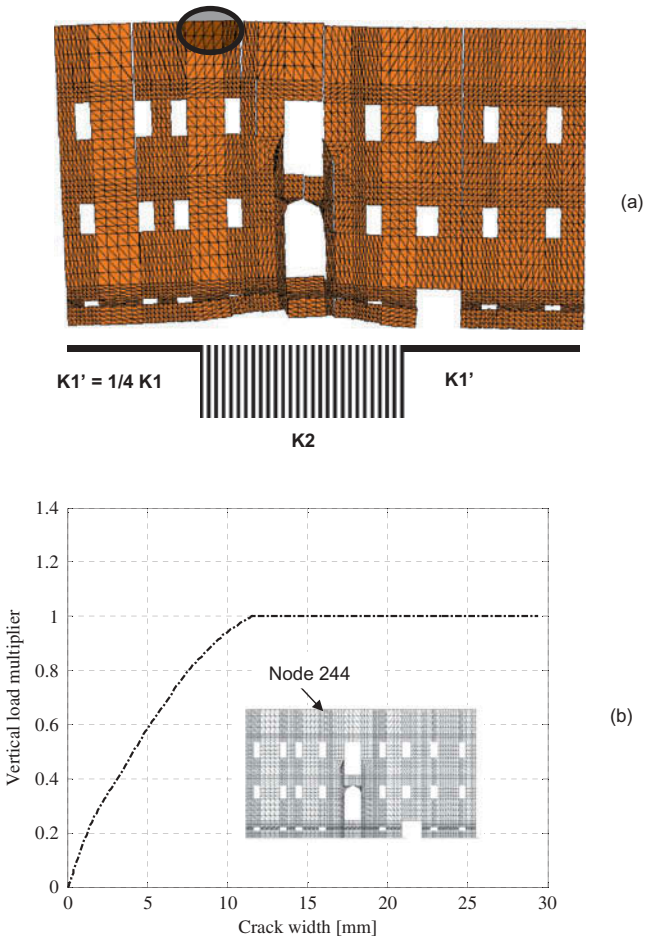

FIG. 23. Prosecution of numerical simulations decreasing linearly K1 to 25% of its initial value: (a) deformed shape of the facade at the end of the non-linear simulations. (6880 triangular elements), (b) crack width versus vertical load multiplier.

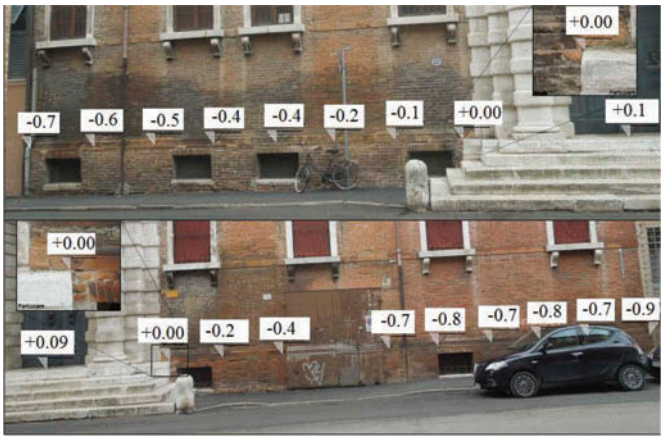

FIG. 24. Measured vertical displacements (in mm) of a horizontal line near the foundation.

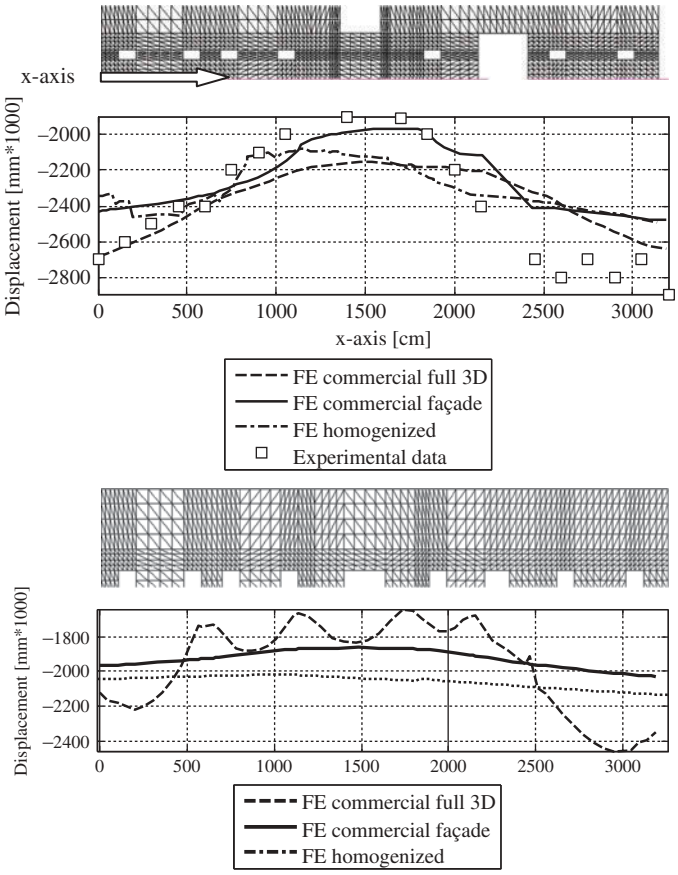

FIG. 25. Comparison among different finite element (FE) models and monitored displacements. Top: base of the building. Bottom: roof level.

parameters needed are chosen in such a way as to match as much as possible the macroscopic behavior of masonry as deduced from the homogenization process.

7. CONCLUSIONS

The crack pattern of the facade of an important historic masonry building, significant example of the Renaissance in Ferrara, was analyzed by means of numerical simulations performed on 2D and 3D FE models with different material behaviors assumed for the masonry—linear elastic, elastic-plastic, non-linear with softening—and by hypothesizing differential settlement of the sub-foundation soil. The results obtained in each type of analysis turn out to be quite close to those measured on-site, both in terms of nodal displacements and in terms of crack–damage patterns. In particular, the parametric analysis carried out in the non-linear homogenized model on the basis of the data surveyed shows that the surveyed crack pattern can be reproduced with a good approximation by choosing properly the stiffness values of the Winkler soil. That approach allows prediction of the structural behavior of a masonry building in the presence of differential settlements and to provide the necessary recommendations and guide lines for specialized and

targeted interventions of conservation and restoration, also for a seismic upgrading of the whole structure. What has been done can be considered a first step of a more complex inverse analysis which would be necessary in order to define a correct stiffness distribution in the Winkler soil, in terms of values and location, on the basis of some known data. The possibility to define the Winkler spring stiffness by solving an inverse problem would allow one to avoid very demanding computational efforts to be handled otherwise within recursive strategies based on iterative processes.

The analysis, at the moment limited to a two-dimensional space, could be extended to a 3D space in order to take into account the out-of-plane movements and related problems. A significant role is played by the multidisciplinary character of the information necessary to set up the initial data the whole analysis should be based on. Historic research, geometric and structural surveys, visual inspections, on-site and laboratory tests, monitored data, all contribute to complete the enormous puzzle representing the past life of an existing building. It is worth noting that each partial result, related to a specific discipline, can be validated only by mutual comparisons with all those provided by the other research fields involved. The proposed models and the adopted analytical procedures, although already known in the literature or already presented by some of the authors, allowed to endorse one of the most likely hypotheses for the damage under consideration, ever recurring in the monitoring carried out so far but never verified until now.

ACKNOWLEDGEMENT

The precious collaboration of the Office of the University of Ferrara in charge of Maintenance and Rehabilitation of the University Estate Heritage in collecting and providing the survey data is highly acknowledged.

REFERENCES

Acito, M., and G. Milani. 2012. Homogenization approach for the evaluation of crack patterns induced by foundation settlement on an old masonry building. *Open Civil Engineering Journal* 6(special issue 1): 215–230.

Alessandri, C., and V. Mallardo. 2012. Structural assessments of the Church of the Nativity in Bethlehem. *Journal of Cultural Heritage*, 13: e61–e69.

Alessandri, C., V. Mallardo, B. Pizzo, and E. Ruocco. 2012. The roof of the Church of the Nativity in Bethlehem: Structural problems and intervention technique. *Journal of Cultural Heritage* 13: e70–e81.

Capurso, M., and G. Maier. 1966. Incremental elastoplastic analysis and quadratic optimization. *Meccanica* 5(2):107–116.

Cervenka, V., L. Jendele, and J. Cervenka. 2007. *ATENA Program Documentation—Part I: Theory*. Prague, Czech Republic: Cervenka Consulting Company. Available at: http://www.cervenka.cz

Circolare 617/09 2009. *Istruzioni per l'Applicazione Nuove Norme Tecniche Costruzioni di cui al Decreto Ministeriale 14 gennaio 2008*. Gazzetta Ufficiale, Rome, Italy: Norme Tecniche Costruzioni.

Ferris, M., and F. Tin-Loi. 2001. Limit analysis of frictional block assemblies as a mathematical program with complementarity constraints. *International Journal of Mechanical Sciences* 43: 209–224.

Giardina, G., A. Marini, M. A. N. Hendriks, J. G. Rots, and F. Rizzardini. 2012. Experimental analysis of a masonry façade subjected to tunnelling–induced settlement. *Engineering Structures* 45: 421–434.

Gikas, V., and M. Sakellariou. 2008. Settlement analysis of the Mornos earth dam (Greece): Evidence from numerical modeling and geodetic monitoring. *Engineering Structures* 30: 3074–3081.

Gilbert, M., C. Casapulla, and H. M. Ahmed. 2006. Limit analysis of masonry block structures with nonassociative frictional joints using linear programming. *Computers and Structures* 84: 873–887.

Grant, R., J. T. Christian, and E. H. Vanmarcke. 1974. Differential settlement of buildings. *Journal of Geotechnical Engineering (ASCE)* 100(GT9):973–991.

Grierson, D. E., A. Franchi, O. De Donato, and L. Corradi. 1979. Mathematical programming and nonlinear finite element analysis. *Computer Methods in Applied Mechanics and Engineering* 17–18(Part 2):497–518.

Holl, M., S. Loehnert, and P. Wriggers. 2013. An adaptive multiscale method for crack propagation and crack coalescence. *International Journal for Numerical Methods in Engineering* 93: 23–51.

Janda, T., M. Sejnoha, and J. Sejnoha. 2013. Modeling of soil structure interaction during tunnel excavation: An engineering approach, *Advances in Engineering Software* 62–63:51–60 [special issue dedicated to Professor Zdenek Bittnar on the occasion of his seventieth birthday: Part I].

Kawai, T. 1978. New discrete models and their application to seismic response analysis of structures. *Nuclear Engineering and Design* 48: 207–229.

Laudiero, F. 2009. *Valutazione e riduzione del rischio sismico del patrimonio culturale. Il caso di Palazzo Contughi–Gulinelli e della Torre Campanaria del Complesso di San Benedetto* [internal report of the Department of Architecture, University of Ferrara]. Ferrara, Italy: University of Ferrara.

Lourenço P. B., and J. Rots. 1997. A multi-surface interface model for the analysis of masonry structures. *Journal of Engineering Mechanics (ASCE)* 123(7):660–668.

Mallardo V. 2009. Integral equations and nonlocal damage theory: A numerical implementation using the BDEM. *International Journal of Fracture* 157(1–2):13–32.

Mallardo, V., R. Malvezzi, E. Milani, and G. Milani. 2008. Seismic vulnerability of historical masonry buildings: A case study in Ferrara. *Engineering Structures* 30(8):2223–2241.

Milani, G. 2011. Simple homogenization model for the non-linear analysis of in-plane loaded masonry walls. *Computers & Structures* 89: 1586–1601.

Milani, G., P. B. Lourenço, and A. Tralli. 2006a. Homogenised limit analysis of masonry walls—-Part I: Failure surfaces. *Computers and Structures* 84(3–4):166–180.

Milani G., P. B. Lourenço, and A. Tralli. 2006b. Homogenization approach for the limit analysis of out-of-plane loaded masonry walls. *Journal of Structural Engineering ASCE* 132(10):1650–1663.

Milani, G., and P. B. Lourenço. 2009. A discontinuous quasi-upper bound limit analysis approach with sequential linear programming mesh adaptation. *International Journal of Mechanical Sciences* 51(1):89–104.

Milani, E., G. Milani, and A. Tralli, A. 2008. Limit analysis of masonry vaults by means of curved shell finite elements and homogenization. *International Journal of Solids and Structures* 45(20):5258–5288.

Milani, G., and A. Tralli. 2012. A simple meso-macro model based on SQP for the non-linear analysis of masonry double curvature structures. *International Journal of Solids and Structures* 49(5):808–834.

Norme Tecniche per le Costruzioni (NTC). 2008. *Nuove norme tecniche per le costruzioni: GU n.29 04/02/2008—14/01/2008*. Rome, Italy: Ministero delle Infrastrutture.

Orduña, A., and P. B. Lourenço. 2005. Three-dimensional limit analysis of rigid blocks assemblages—Part I: Torsion failure on frictional joints and limit analysis formulation. *International Journal of Solids and Structures* 42(18–19):5140–5160.

Padura, A. B., J. B. Sevilla, and J. G. Navarro. 2012. Settlement predictions, bearing capacity and safety factor of subsoil of Sevilla's Giralda. *International Journal of Architectural Heritage* 6: 626–647.

Skempton, A. W., and D. H. MacDonald. 1956. The allowable settlements of buildings. *ICE Proceedings: Engineering Divisions* 5(6):727–768.

Strand 7. 2004. *Straus 7.2: User's manual*. Sidney, Australia: Strand 7. Available at www.strand7.com

Torboli, M. 1999. Il "Magnifico Palagio" Contughi–Gulinelli di Ferrara: Per la storia di una dimora patrizia. *Musei Ferraresi* XVIII, 77–90.